No:72 Desember 1988

CALIBRATION OF AN ULTRASONIC CURRENT METER

by

Eirik Sørgård, Thomas Martinsen
and Eyvind Aas

INSTITUTT FOR GEOFYSIKK

UNIVERSITETET I OSLO

INSTITUTE REPORT SERIES

No:72 Desember 1988

CALIBRATION OF AN ULTRASONIC CURRENT METER

by

Eirik Sørgård, Thomas Martinsen
and Eyvind Aas

ABSTRACT

The calibration of velocity, temperature and salinity measured with the ultrasonic current meter UCM-10 is described. The calibrated velocities differ from those given by the manufacturer. Contribution to the Reynolds stress $-\varrho\overline{u'w'}$ from the turbulence produced by the instrument itself seems to be negligible for mean velocities less than 1 ms^{-1}. Oscillations in the form of periodic twisting and tilting of the instrument have little influence on $-\varrho\overline{u'w'}$, but are more important for the other Reynolds stresses. A constant transverse tilt of the instrument during the measurements may influence the recorded stresses significantly.

CONTENTS

1. INTRODUCTION

Around 1975 an ultrasonic current meter was constructed by T. Gythre (1976), with the possibility of recording turbulent velocity fluctuations along three axes. Later on, when the instrument was produced for commercial sale by the company Simrad Optronics, Oslo, the construction was changed so that the 10 Hz recordings were averaged to give 1 Hz values, since most of the customers were only interested in mean values.

In 1986 it was decided at the Institute of geophysics to convert the instrument UCM-10 back to its original condition, and to see if the turbulent Reynolds stresses could be recorded with sufficient accuracy in marine environments. During the work it was found necessary to calibrate the different sensors of the instrument, and to see if the instrument recorded any self-generated turbulence.

Calibration of the instrument and turbulence measurements in the estuary of Glomma have been described in a thesis by Sørgård (1988), while a thesis by Martinsen (1988) describes the electronics of the instrument and the turbulent friction between sea ice and the water below. An abridged description of the estuarine measurements has been worked out earlier (Sørgård et al. 1988), while an abridged description of the calibrations and the problems of measurement is presented here.

The production of the UCM instruments has now been taken over by the company Bergen Ocean Data, and a new model, UCM-40, where several earlier shortcomings have been eliminated, is ready for the market. The UCM-10 will not be produced any more. Although our results refer to a specific rebuilt instrument of the old model, the methods of calibration and measurements that were used should be of general validity.

2. UNCERTAINTY OF A MEASUREMENT

We shall assume that the water which surrounds a sensor has the

true value X of a quantity, while the measured value is x. The purpose of the calibration is to find a relation between X and x, so that X can be estimated from the recorded value of x. Here we shall only apply linear relations, which give X as

(2.1) $X = A + Bx$,

where A and B are calibration constants to be determined. In the ideal case A is zero and B is 1.

When X is constant, the mean value x_m will be obtained from a series of repeated measurements. From different values of X and corresponding different values of x_m, A and B will be found by the method of least squares.

Some of the sensors need a certain time to adjust to the changes in the quantity they measure. The response time is the time needed by the sensor before the measured change Δx has reached a certain percentage of the true change ΔX.

The power of resolution dx is the lower limit of a small change of the quantity that the instrument will detect and record.

The offset value Δx_0 is a constant that may be subtracted from the recording x', so that the measured mean value of x becomes zero when the true value X is zero. The offset value is found from

(2.2) $\Delta x_0 = [x'_m]_{X=0}$.

Measured x is then defined as

(2.3) $x = x' - \Delta x_0$.

In some cases it may be convenient to introduce the offset value, in other cases it will be more practical to let it become a part of the calibrated relation (2.1) between X and x.

Different series of measurements may give different values of Δx_0. The standard deviation of these values will give a measure of the

uncertainty of the offset value, s_Δ:

$$(2.4) \quad s_\Delta = \overline{[(\Delta x_0 - \overline{\Delta x_0})^2]}^{1/2} \ .$$

The overbar denotes the mean value of the results of different series. (Note that the index m denotes the mean value of a single series with constant conditions).

The repeatability (or precision) of the measured x is the standard deviation s_x when the true value X is constant:

$$(2.5) \quad s_x = [(x-x_m)^2{}_m]^{1/2}_{X=\text{const.}} \ .$$

When the line (2.1) is found, the absolute uncertainty of our estimated mean values of the quantity may be expressed as the rest deviation s'_X between the line and the true X values:

$$(2.6) \quad s'_X = \overline{[(X-(A+Bx_m))^2]}^{1/2} \ .$$

Sometimes the rest deviation in relative units is a better way to express the uncertainty. It is defined as

$$(2.7) \quad s'_{Xr} = \overline{[(1-((A+Bx_m)/X))^2]}^{1/2} \ .$$

When the number N of datapoints is small, the parentheses in (2.6) and (2.7) should be multiplied with $[N/(N-2)]^{1/2}$, and the parentheses in (2.4) and (2.5) should be multiplied with $[N/(N-1)]^{1/2}$.

The absolute uncertainty of X based on a single measurement of x may be estimated as

$$(2.8) \quad s_X = [s_x^2 + s'^2_X]^{1/2} \ .$$

The lower limit for s_X, however, should be either s_Δ, if the offset value has been applied, or the resolution dx.

The standard deviation of x_m is statistically estimated as

(2.9) $s_{xm} = s_x'/\sqrt{N}$,

where N is the number of observations from which x_m is calculated. When N is a large number, s_{xm} will become very small. However, in practice the absolute uncertainty of x_m will depend on the calibration, and a better estimate of s_{xm} is

(2.10) $s_{xm} = [(s^2{}_x/N + s'^2{}_X]^{1/2} \approx s'_X$.

This value should not be less than the uncertainty of the offset value or the power of resolution.

3. THE INSTRUMENT

3.1. General description

The properties of the ultrasonic current meter UCM-10 and its different sensors will be described in this chapter, while the way this properties were calibrated will be explained in Chapter 4. The instrument measures water velocity along three axes. The shortest sampling intervall possible is 0.096 seconds, corresponding to approximately 10 sets of measurements per second. The instrument is also equiped with a compass which relates the orientation of the instrument to magnetic north, and sensors for salinity, pressure and temperature. The current meter consists of a cylinder with the sensors fixed to the lower end. The height of the current meter is 80 cm, the diameter of the cylinder 12 cm, and the diameter around the velocity sensors about 20 cm (Fig. 2a).

The instrument gives an analoge voltage as a linear function of the measured parameter. The setting up for recording is shown in Fig. 1. Analoge signals are sent from the instrument via a parallel sheltered cable to a interface containing an analoge-to-digital converter. Power supplies for the interface and the instrument are two 18 V battery packages. The digital signals are sent to a battery driven portable micro computer, and the data are stored on its 1 Mb hard disk. With a measuring frequency of 10 Hz

data for 1.5 hours can be stored on the hard disk. The data transfer is controlled by software on the micro computer. The diskette station enables us to transfer the data to 3.5'' diskettes.

3.2. Velocity sensors

Each of the three axes of measurement are equiped with two 4 MHz crystals. They are excited simultanously with 300 V, and acoustic waves are sent out. The crystals change from transducers to receivers, and the time the waves use in both directions along the path between the crystals are measured. The time used from A to B (see Fig. 2b) is

$$(3.1) \qquad T_{AB} = \int_A^B 1/(c+v\cdot\cos 45^0)\, dL/\cos 45^0 \ ,$$

where c is the speed of sound in water, v is the velocity of the water in the measuring direction, and $dL/\cos 45^0$ is the path increment along the path from crystal A to crystal B. Similarly the time used from B to A becomes

$$(3.2) \qquad T_{BA} = \int_B^A 1/(c-v\cdot\cos 45^0)\, dL/\cos 45^0 \ .$$

Since $|c| >> |v|$, the ratio in parenthesis of equations (3.1) and (3.2) may be expanded in series.

If c and v are substituted with their mean values $\bar{c}$ and $\bar{v}$, the integration may be performed, and we get the following approximated expression for the time difference, ΔT:

$$(3.3) \qquad \Delta T = T_{AB} - T_{BA} = 2\bar{v}L/\bar{c}^2 \ ,$$

where L is the horizontal length between the crystals (Fig. 2b). The theoretical power of resolution of the velocity sensor is 1 mm/s. L is 14 cm, and with c=1500 m/s equation (3.3) shows that ΔT=0.12 ns. In order to measure such short time differences the sensor uses a sweepgenerator, activated by the first wave (signal) and deactivated by the last one. The amplitude from the sweepgenerator is then proportional to ΔT. Simultanously the total

time of the fastest wave is measured with a 1 MHz counter. The counter is blanked before the excitation of the crystal, and starts with the excitation. The speed of sound is then approximately given by

(3.4) $\bar{c} = L'/(N \cdot 10^{-6} \text{ seconds})$,

where N is the counters value when the wave arrives at the receiver, and L' is the total path given by $L'=L/\cos(45^0)$. The uncertainty in c due to the resolution of the 1 Mhz counter is 1% and may at most give an uncertainty of 2% in the measured velocity. After every measurement of the quantities a measurement of zero velocity is simulated to detect eventual drift in the electronics. The drift is corrected with a resolution of 1 mm/s. The correction is made by short-circuiting the output to the crystals so $\Delta T=0$, and by comparing the result with the similar measurement one time step earlier. (However, by this technique a change in the crystals will not be detected.) When these effects are taken into account the velocity is given by

(3.5) $v = (\bar{c}^2/2L)\Delta T = C \cdot \Delta T$, $\qquad C = \bar{c}^2/2L$,

where C is a constant varying from measurement to measurement depending on the speed of sound. The velocity is measured with the same technique in all three directions, but in the vertical there is no reflector. The horizontal velocities are mean values along paths of total length 20 cm, while the vertical velocity is the mean value along a path of length 14 cm.

The UCM-10 has no moveable parts and consequently it is the electronics that limits the response time, which is far less than the minimum sampling intervall of 0.1 seconds. The velocity data are registered with a theoretical resolution of 0.24 cm/s, but in practice the repeatability will give the lower limit of resolution between velocities. For the horizontal velocities the repeatability was found to be 0.4 cm/s and for the vertical 0.5 cm/s. The uncertainty of the offset value was found to be slightly smaller:

$s_{\Delta u}$ = 0.3 cm/s , $s_{\Delta v}$ = 0.3 cm/s , $s_{\Delta w}$ = 0.4 cm/s .

The absolute uncertainty of the time averaged vertical velocity is 16%, and for the time averaged horizontal velocities we found that small and large values are less accurate than moderate ones, i.e.:

0.0 ≤ |u|,|v| < 15.7 [cm/s] => absolute uncertainty 9% ,
15.7 ≤ |u|,|v| < 74.8 [cm/s] => absolute uncertainty 3% ,
74.8 ≤ |u|,|v| [cm/s] => absolute uncertainty 8% .

3.3. Temperature sensor

A Fenwall termistor (K5174) is used for temperature measurements. The termistor is an electric resistance changing in value as a linear function of temperature. The sensor is able to measure temperatures in the range -5 to +45 ^{0}C, with a resolution of 0.1 ^{0}C. The response time is 5 seconds to reach 63% of the true change, and 25 seconds to reach 99.5%. The repeatability of the sensor was found to be 0.12 ^{0}C, while the absolute uncertainty of the mean value was found to be 0.1 ^{0}C.

3.4. Pressure sensor

The pressure is measured with a piezoelectric crystal (Kistler 4043/A10), and its range is $0\text{-}10 \cdot 10^5$ Pa (0-90m depth). The response time is far less than the shortest sampling intervall of 0.1 seconds. The resolution is 10^3 Pa (10 cm in depth) and the absolute uncertainty is about $2.5 \cdot 10^3$ Pa (25 cm in depth). It is the resolution that limits the accuracy of the sensor in practical use, because the uncertainty of the sensor to a great extent is a constant part of the pressure. The repeatability of this sensor was found to be $0.5 \cdot 10^3$ Pa (5 cm in depth).

3.5. Conductivity sensor

The conductivity is measured by an inductive cell (Aanderaa 2103), containing two spools. During the measurement the primary spool receives an alternating voltage of 3V and the induced voltage in the secondary spool will be proportional to the conductance of the water. When the instrument starts measuring it will reach its correct value after about 0.025 seconds, and afterwards it will

register the change in the conductance with a response time of 0.0025 seconds. The resolution is 0.08 mMho, corresponding to 0.08 practical salinity units with a salinity of 10, and 0.09 with a salinity of 20, when the temperature is 15 ^{0}C and the pressure 1 atmosphere. The mean salinity was found to have an absolute uncertainty of:

0.07 for $S \leq 2.8$
0.26 for $S > 2.8$

The repeatability was found to be 0.8.

3.6. Compass

The UCM-10 current meter is equiped with a compass (Aanderaa 1248), which gives the orientation of the instrument relative to magnetic north. When the measurement starts, the compass needle is locked in a fixed position and the compass turned. The needle hits a potensiometer ring and the voltage drop over the potensiometer ring is a function of the compass course. This measurement is made only every tenth second. The resolution of the compass course is 2^{0} and the absolute uncertainty 5^{0}.

3.7. Data transfer and logging

The seven analoge voltages representing the seven parameters measured, are sent from the instrument to a interface containing a channel selector (multiplexer), an A/D-converter and a voltage modulator. Each of the analoge entrances have addresses that enables the data logger to decide which parameter that should be read. When the interface receives the signal from the data logger, the chosen analoge voltage is transformed to a binary number presented in parallel at the output together with the address. The A/D-converter is based on the method of successive approximations, and converts the analoge voltage to two 8 bit numbers where four of the bits are used to represent the address. The 12 bits left to represent the voltage give a resolution of 4.89 mV, because the voltage domain of the A/D-converter is ±10V.

The representation of the converter is:
-10V : 0 (2^{0}-1) , 0V : 2047 (2^{11}-1) , 10V : 4095 (2^{12}-1)

The signals representing the seven measured parameters are given in voltage by:

Velocity : -5V : -2.5m/s , 0V : 0m/s , 5V : 2.5m/s

Temperature : -5V : -5 ^{0}C , 0V : 20 ^{0}C , 5V : 45 ^{0}C

Pressure : -5V : 0 atm. , 0V : 5 atm. , 5V : 10 atm.

Conductivity: The conductance y of the water is found from the voltage x of the sensor by:

$$y(\text{mMho}) = 0.75(\text{mMho}) + 13.95(\text{mMho/V}) \cdot x(\text{V})$$

Compass : 0V : 0^{0} , 5V : 360^{0}

The data logger chosen for our measurements was an EDDA CPC micro computer manufactured by Comdel a/s, Bergen. This is a suitable logger for field measurements, because it is portable, water resistent, able to work 24 hours by its own battery supply, and able to communicate with and direct the A/D converter via a parallel port. The data logger is equiped with a 1024 kb hard disk memory, where 840 kb is available for data storing. By a 10 Hz sampling frequency we are able to measure continuously for 100 minutes before transfering the data to a diskette by a SONY HBD50 diskette station.

The task of the data logger is to communicate with the immersed instrument, direct the A/D converter, present the measured values on the computer screen, and store the data in files. The soft-ware controlling the data transfer also enables us to vary the sampling intervall between 0.1 and 4 seconds.

3.8. Power supply

The power supply to the instrument and the interface are two 18V battery packages. The power consumption is approximately 3.2 W for the current meter and 1.2 W for the interface. The signal ground from the instrument is connected to the negative voltage supply from the battery to the interface, so that the signal voltages refer to the same potential. The negative potential of the cable which supplies power to the instrument can not be used as ground because the cable will have a varying voltage drop along it, depending on the electric current passing through the cable. Signal ground is connected to the shelter of the signal cabel,

which is coupled to environmental earth during the measurements (Fig. 3).

4. CALIBRATION

4.1. Calibration of the velocity sensors

4.1.1. The offset error of the velocity

Changes in the crystals are not corrected for during the measurements, contrary to changes in the speed of sound and drift in the electronics. The effect of the crystal temperature was investigated by measuring in a vessel with zero flow during one minute for each different temperature. Two measurements were made elsewhere and with longer record length. The one marked '*' in Table 1 is from the Marintek tank, and the record length was 5 minutes. The one marked 'o' is from an ice-covered pond with no flow, and the record length was 10 minutes. The results are listed in Table 1.

The offset values for the different axes are plotted in Fig. 4.a-4.c as functions of temperature. As we can see there is no clear relation between the change in offset value and the temperature. The mean offset value has therefore been used for each axis:

x-axis: $\Delta u_0 = -1.1$ cm/s , $s_{\Delta u} = 0.3$ cm/s ,
y-axis: $\Delta v_0 = -0.6$ cm/s , $s_{\Delta v} = 0.3$ cm/s ,
z-axis: $\Delta w_0 = -0.6$ cm/s , $s_{\Delta w} = 0.4$ cm/s .

The uncertainty s_Δ of the offset value is defined by eq. (2.4). No significant drift during the experiments was detected.

4.1.2. Calibration of the vertical velocity sensor

The calibration was made onboard R/V Trygve Braarud in Oslofjorden. The instrument was lowered with constant speed from the surface to 20 m depth while the time was measured, and thereby the true vertical velocity could be estimated. The same procedure was followed while the instrument was hauled from 20 m depth to the surface (marked '*' in Table 2.). The data are presented in

Table 2, and the values are corrected for their offset error.

Rather than seeking a relation of the form $W=A+Bw'_m$, where w'_m is the mean measured velocity and A and B are constants to be determined, the earlier found offset value Δw_0 was first subtracted from the observations, and the difference termed w_m. The constant B of the relation $W=B \cdot w_m$ was then determined by the method of least squares. This method was chosen because the earlier offset measurements were believed to be more accurate than the data achieved by lowering and hauling the instrument, so that Δw_0 is more accurate than the value of A would have been.

The most important source of uncertainty in this calibration lies in the measured velocity w'_m, because the instrument may not have had a complete vertical orientation on its way through the water. If the instrument is tilted, only the velocity component parallel to the vertical sensor will be recorded as vertical speed, and horizontal currents may influence the result. However, this error has been assumed small since no tilt of the instrument was observed during the measurements. (The error due to associating a pressure change of 10^5 Pa with a vertical displacement of 10m is minor and negligible).

It was not found necessary to separate the positive and negative values of the vertical velocity. The calibration curve for the vertical sensor is based on the data for $w_m < 60$ cm/s. This results in a calibration curve for W like:

(4.1) $W = 1.70 \cdot w_m$.

The rest deviation, that is the root-mean-square difference between W and the curve (eq. 2.6), is $s'_W=2.9$ cm/s.

The calibration curve and the data are plotted in Fig.7. It can be seen from Fig.7 that the values are more spread from the curve when they increase in absolute value. A better way to estimate the rest deviation may then be to scale all the deviations by their corresponding "true" values (eq. 2.7). In this way the absolute uncertainty for W in relative units was found to be 16%.

It can be seen from Fig. 7 that the two greatest values for w_m lie somewhat off the calibration curve. We have, however, chosen to use the calibration curve found for values of $w_m < 40$ cm/s, also for observations larger than 40 cm/s, rather than to use the dotted line of Fig. 7. This choice is supported by another result. As described later the calibration curve U and V will depend on the calibration curve for W. If we take into account the two largest values for w_m, i.e. use the dotted calibration curve, and estimate the true horizontal values U and V, they will lie far off the calibration curve which the other values seem to indicate. This is shown in Fig.8. If, on the other hand, we use the hatched calibration curve based on the values for $w_m < 40$ cm/s, these u and v values will also fit into the calibration curve indicated by the other values. Thus it seems reasonable to apply equation 4.1 on all observed vertical velocities.

4.1.3. Measurements for the calibration of horizontal velocity

The calibration measurements took place in Marinteks tank in Trondheim. The tank is 80 m long, 10 m wide and 6 m deep. The instrument was mounted on a lorry of the same width as the tank and of 5 m length. The vertical distance from the lorry to the water surface was about 1 m. By dragging the instrument with different speeds through water at rest, we were able to investigate both the measured speed as compared with the speed of the lorry, and the turbulence generated by the instrument itself.

Five series was measured with different suspensions and with speeds from 5 cm/s to 150 cm/s:

A) The instrument was suspended to a wire with the top of the instrument 30 cm below surface. A rudder was used to keep the instrument stable against the passing waters (Fig. 5.a).

B) The same suspension was used as in series A, but with the top of the sensor 210 cm below the surface.

C) The same suspension was used as in series B, but without the rudder (Fig. 5.b).

D) A frame of two angle irons was suspended to the instrument and to a beam on the lorry. The top of the sensor was 130 cm below

surface (Fig. 5.c).
E) The same suspension was used as in series D, but the position of the vertical velocity sensor was changed, i.e. rotated 180^0 in the horizontal plane (Fig. 6a,b).

The position of the vertical velocity sensor in series A-D was before the instrument with regard to the current, and about 45^0 from the direction of the current (Fig. 6a). With this orientation we belive that the vertical velocity sensor is least influenced by the instrument. Measurements made by Oceanor (Kolstad, 1985), shows that also the horizontal velocity is best recorded with this orientation.

We were not able to keep the instrument steady during the measurements. When it was suspended to the wire we had oscillations in the direction of the mean stream up to a velocity of 30 cm/s. The amplitude of this oscillation was estimated to 5-10 cm. For speeds above 30 cm/s the dominating movements of the instrument seemed to be oscillations in the transversal direction with a maximum amplitude of 10-15 cm. The sensor also obtained a constant tilt in the direction of the mean stream with increasing velocity.

To some degree the oscillations were damped with the frame of angle iron, but for speeds above 70 cm/s the instrument oscillated in the transversal direction. Maximum amplitude was registered at a speed of 90 cm/s and estimated to 10 cm. The two last measurements of series D (100 cm/s, 150 cm/s) were taken with an improved mounting, where the angle irons were suspended to an additional beam on the lorry. The oscillations were then less than 10 cm. Series E was measured with this improved mounting.

The mean velocities given by the instrument differed from the velocities of the lorry, and closer analysis of the recordings were necessary in order to calibrate the instrument.

4.1.4. Analysis of recorded horizontal velocities

By first calibrating the vertical velocity sensor we were able to use the data from the tank to calibrate the horizontal velocity

sensors. It was necessary to calibrate each direction separately because they might have different calibration constants, and because a separation of the directions is necessary for turbulence studies. The compass did not work in the tank, and the calibration was performed as described below.

The following notations are used:
U_l : the speed of the lorry.
u_m, v_m, w_m : measured mean velocities along the x-,y- and z-axis of the instrument, respectively.
U, V, W : true mean values along the three axes.

1) The vertical velocity is calibrated separately, and for a measured value w_m we can find the true value W.
2) The true velocity along the x-y plane of the instrument is then given by:

$$(4.2) \quad \sqrt{(U^2 + V^2)} = \sqrt{(U_l^2 - W^2)}.$$

3) We then estimate the angle between the instruments x-axis and the direction of the mean flow by:

$$(4.3) \quad \varphi = \arctan(v_m/u_m) .$$

4) This angle is used to decompose $\sqrt{(U^2+V^2)}$ along the x- and y-axis:

$$(4.4) \quad U = [\sqrt{(U^2+V^2)}]\cdot\cos\varphi , \qquad V = [\sqrt{(U^2+V^2)}]\cdot\sin\varphi .$$

5) Now the true values U and V are known, and the calibration curves may be formed by plotting these values as functions of u_m and v_m.

The obvious inaccuracy of this method results from point 3, where the angle φ is estimated. This angle may differ from the true angle if U and V have different calibration curves. Even if they have the same calibration curve the angle may be estimated wrong, if u_m and v_m differs in magnitude and the curve is nonlinear.

The problem may to some extent be compensated for by successive approximations in the determination of φ. The values U and V may be substituted for u_m and v_m in eq. (4.3). The new value of φ results in new calibration curves for U and V, the new curves may be used to estimate a better value of φ again, and so on until these series converge towards fairly constant values of φ, U, and V.

4.1.5. Calibration of the horizontal velocity sensors

The measured values u'_m and v'_m were corrected for the offset error to give u_m and v_m before the angle φ was calculated. The "true" horizontal velocities U and V were calculated from the speed U_l of the lorry by eqs. 4.2-4.4. The resulting calibration curves for U and V were now found to coincide. We therefore saw no reason to distinguish between these velocities, and it was also found unnecessary to distinguish between positive and negative values. The fact that the two calibration curves coincided may to some degree be a result of the calculated angle φ which results in:

$$(4.5) \qquad \frac{V}{U} = \frac{\sin\varphi}{\cos\varphi} = \frac{v_m}{u_m} ,$$

i.e. the ratio between the measured and the true values is the same for each measurement. This is not equivalent with having coinciding calibration curves, but the values are not truly independent. However, it is reasonable that they have the same calibration curve since the measurements are based on the same type of sensor with the same electronics.

Apart from the uncertainty in W, the main uncertainty of this calibration method is the calculated angle φ, as was pointed out in the preceding section. Since the x- and y-direction seem to have the same calibration curve, this error will be reduced, however, because if V is calculated too large, then U will be calculated too small and vice versa (Fig. 9). Since the calibration curve is estimated with the method of least squares, the line will lie between the U and V points and closer to the correct calibration curve.

On this basis we have tried to reduce the error further by the method of successive approximations, as described in section 4.1.4.

In our case the procedure was repeated four times. The values are listed in Table 3 and plotted in Fig. 10.

The calibration curve was divided into four linear parts:

$$
\begin{aligned}
(4.6)\quad & 1)\ U = 1.51 \cdot u_m , && 0.0 \leq u_m < 10.4 , \\
& 2)\ U = 5.5 + 0.98 \cdot u_m , && 10.4 \leq u_m < 35.5 , \\
& 3)\ U = 12.6 + 0.78 \cdot u_m , && 35.5 \leq u_m < 79.8 , \\
& 4)\ U = -28.1 + 1.29 \cdot u_m , && 79.8 \leq u_m ,
\end{aligned}
$$

where the velocities are in cm/s. Identical expressions give V as a function of v_m.

Curve 1) is forced to pass through origo (0,0). This is done because we have already subtracted the offset value from the observations. The rest deviation from the curves, s´, was found to be:

$$s'_1 = 0.7 \text{ cm/s} , \quad s'_2 = 1.0 \text{ cm/s} , \quad s'_3 = 1.5 \text{ cm/s} , \quad s'_4 = 4.6 \text{ cm/s}.$$

The relative rest deviation was:

$$s'_{r1} = 9\% , \quad s'_{r2} = 3\% , \quad s'_{r3} = 3\% , \quad s'_{r4} = 8\% .$$

The uncertainties above are significantly larger than the proclaimed error in the speed of the lorry, which was 0.5 cm/s, independent of the speed.

4.2. Calibration of the temperature sensor

The temperature sensor was calibrated by starting with the instrument immersed in a vessel of cold water, removing cold water and adding hot water, stiring to a homogeneous water mass and measuring the temperature. The temperature in the vessel was also measured with a thermometer with an error of 0.05 ^{0}C. The reading

of the thermometer had a possible error of 0.1 ^{0}C. A measurement at 0 ^{0}C was made in a volume of water mixed with ice. The data are listed in Table 4, and plotted in Fig. 11. A rest deviation of 0.07 ^{0}C was obtained from the calibration curve given by:

(4.7) $T = 0.2^0C + t_m$,

where T is the true value and t_m the mean value of the measured temperature. The deviation is of the same order as the uncertainty due to the reading of the thermometer.

4.3. Calibration of the salinity sensor

The salinity sensor was calibrated by:

1) Measuring the salinity in a vessel with known volume V_1, density ϱ_1, and salinity S_1.
2) Removing a volume V_2 of the salt water.
3) Adding a volume V_3 of fresh water with density ϱ_3.
4) Mixing the watermasses until a homogeneous watermass was obtained in the vessel, with salinity S and density ϱ. The volume in the vessel was now V.
5) Measuring the new salinity S in the vessel.

The procedure was repeated from point 2) to 5) until a satisfactory amount of data was obtained. All measurements were made with a frequency of 10 Hz, and a record length of 1 minute. The salinity S was calculated from the salt and mass budgets:

(4.8) Salt budget: $\varrho_1 S_1 V_1 - \varrho_1 S_1 V_2 = \varrho SV$,

(4.9) Mass budget: $\varrho V = \varrho_1 V_1 - \varrho_1 V_2 + \varrho_3 V_3$.

The following equation for S was then obtained:

(4.10) $$S = S_1 \frac{V_1 - V_2}{(V_1 - V_2) + V_3 \varrho_3 / \varrho_1}$$.

The results are shown in Table 5, and plotted in Fig. 12.

It was found convenient to split the calibration curve in two

linear parts. In addition to the values listed in Table 5, we had 24 measurements in fresh water that gave a mean salinity of 0.32. These 24 values and the lowest value from Table 5 formed the data set for the calibration curve for measured values below 1.32. If S denotes the true value and S_m the measured mean value, the calibration curves become:

$$(4.11) \quad S = -0.88 + 2.793 \cdot S_m , \quad 0.0 \leq S_m < 1.32 ,$$
$$S = 1.49 + 0.997 \cdot S_m , \quad 1.32 \leq S_m ,$$

where the salinities are in practical salinity units.
The rest deviation was found to be 0.26 for the upper part of the calibration curve and 0.07 for the lower part. The starting salinity S_1 was measured with a laboratory salinometer with uncertainty about 0.01.

4.4. Noice from the electronic system

All parameters were measured ten times a second for 5 minutes in still water in order to get an estimate of the total noice from the electronic system. All values were corrected with their calibration curves. The following standard deviations were achieved and may be considered as the mean deviations caused by the electronic noice:

$s_u = 0.43$ cm/s , $s_v = 0.40$ cm/s , $s_w = 0.50$ cm/s ,
$s_T = 0.12\ ^0C$, $s_S = 0.79$, $s_p = 5 \cdot 10^2$ Pa .

Indices T,S and p refer to temperature, salinity and pressure, respectively, and u, v and w to the velocities.

We note that the measurements were made with only one set of fixed conditions. With different conditions the standard deviations may become different. However, we believe that the estimates above give the correct order of magnitude of the repeatability, that is the error due to electronic noice.

The standard deviations listed above are supposed to represent the standard deviation of a single measurement, but the absolute uncertainty of a single measurement should also take into account

the uncertainty of the calibration, as expressed by eq. 2.8. The absolute uncertainty of our mean values, however, is practically not influenced by electronic noice at all, as shown by eq. 2.10.

5. TURBULENCE MEASUREMENTS

5.1. Effect of electronic noice on turbulent transports

An estimate of the influence on the turbulent transport parameters from the electronic noice may be the different correlations achieved from the same series, as were discussed in the preceeding section:

$\overline{u'u'} = 0.18$,	$\overline{u'v'} = 0.02$,	$\overline{u'w'} = -0.07$,	$[cm^2/s^2]$
$\overline{v'v'} = 0.16$,	$\overline{v'w'} = -0.03$,	$\overline{w'w'} = 0.25$,	$[cm^2/s^2]$
$\overline{u's'} = 4 \cdot 10^{-3}$,	$\overline{v's'} = -0.04$,	$\overline{w's'} = -0.02$,	[cm/s]
$\overline{u'T'} = 9 \cdot 10^{-3}$,	$\overline{v'T'} = 6 \cdot 10^{-3}$,	$\overline{w'T'} = 0.01$.	$[cm/s \cdot {}^0C]$

We see that the auto-correlations to some degree are influenced by the electronic noice, while the influence on the cross-correlations is negligible.

5.2 Turbulence generated by the instrument itself

The values of the turbulent momentum transports, which were recorded while the instruments was dragged through the test tank at Marintek, are listed in Table 6, and $\overline{u'w'}$ is plotted in Fig.13 and Fig. 14 as a function of the mean velocity. The velocities refer to the coordinate system which will be described in Chapter 6. All values are corrected by the calibration curves.

The values of $\overline{u'w'}$ are of most interest to us, and we shall discuss them more closely. The data seem to indicate that the different suspensions result in different contributions to $\overline{u'w'}$. It should be noted that the effects of the movements of the instrument during the measurements and the electronic noice is included in the recordings.

In series E we observe that at a speed of 50 cm/s the instrument records a relatively large value for $\overline{u'w'}$. In this series the vertical sensor was positioned behind the instrument, with regard

to the mean flow (Fig. 6b), and has probably been strongly influenced by the turbulence produced by the instrument. The values of the other series, where the vertical sensor was positioned before the instrument, are far less at the same speed. From this we may conclude that the vertical sensor should be positioned before the instrument during turbulence measurements, in order to avoid self-generated contributions to the calculated Reynolds stresses.

In the different series A-D $\overline{u'w'}$ shows the same tendency when U increases from 0 to 70 cm/s (Fig. 13-14). The negative value of $\overline{u'w'}$ increases when U increases from 0 to 30-40 cm/s, and decreases in negative value towards zero when the velocity approaches 60 cm/s. Between 60 and 70 cm/s $\overline{u'w'}$ becomes positive. From 70 cm/s and upward $\overline{u'w'}$ seems to depend on the type of instrument suspension. The values for $\overline{u'w'}$ in series D (angle iron frame) increase when U increase from 70 cm/s to 150 cm/s, while the values for series A-C (wire suspension) decrease when U increases towards 100 cm/s, but are positiv and in the same range as series D at a speed of 150 cm/s.

The values of $\overline{u'w'}$ with an angle iron suspension are throughout less in absolute value than the values from the wire suspension. This is evidently due to the fact that with the angle iron suspension the movements of the instrument are less, and that the instrument stood perpendicular to the mean flow, while the instrument was tilted in the direction of the mean flow with the wire suspension. The tilt increased with increasing speed. This last effect may affect the self-generated turbulence.

It should be noted that the values discussed above are measurements of self-generated turbulence when the water flow is non-turbulent. They only serve as an estimate of what the self-generated turbulence might be in the case of real turbulent flow.

5.3. The effect of measurements over finite distances

The horizontal velocity measurements are mean values in space

along a total path of 20 cm, while the vertical velocity is measured along a 14 cm path (Fig. 2a,b). The distance between the centres of horizontal and vertical paths is about 10 cm. Our estimates of the Reynolds stresses are based on the assumption that the horizontal and vertical velocities at all times are fairly constant within the area or the box that the sensors define. Turbulence on the same scale as the box or on a smaller scale will only be partly registered, or not registered at all.

Soulsby (1980) has estimated the loss of registered turbulence due to this effect. We designate D as the length scale of the box, λ as the length scale of turbulence, and τ as the time scale of turbulence. They are related by Taylor's hypothesis:

(5.1) $\lambda = U \cdot \tau$,

where U is the mean velocity of the flow.

Soulsby states that:
90% of the turbulence with length scale $\lambda = 6.0 \cdot D$ is registered,
50% of the turbulence with length scale $\lambda = 2.2 \cdot D$ is registered,
0% of the turbulence with length scale $\lambda \leq 1.4 \cdot D$ is registered.

With a mean velocity of 60 cm/s and a box dimension of D=20 cm none of the turbulence components with periods less than 0.5 seconds will then be registered.

6. PROBLEMS IN FIELD MEASUREMENTS

6.1. Velocities defined relative to the mean stream line

In practice it is difficult to keep the instrument vertical during the measurements. The instrument may tilt in the direction of the mean flow and/or in the transversal direction (Fig. 15). The UCM-10 has no tilt sensor, and in our work the data has therefore been related to the mean stream line. The axes of the instrument are denoted x',y' and z', and the corresponding velocities are denoted u',v' and w'.

In the new coordinate system x,y,z we require that $v \equiv 0$ and $w \equiv 0$, i.e. the x-axis is parallel to the mean stream line through the point of measurement. The instrument measure a compass course giving the angle α between magnetic north and the instruments positive x-axis. In order to compensate for a changing orientation of the instrument, we will first of all define a coordinate system x_n, y_n, z_n relative to magnetic north (Fig. 16a). The velocities relative to the new coordinate system are defined by:

$$\theta = \pi/2 - \alpha \quad (6.1)$$

$$u_n = u' \cdot \cos\theta - v' \cdot \sin\theta \quad (6.2)$$

$$v_n = u' \cdot \sin\theta + v' \cdot \cos\theta \quad (6.3)$$

$$w_n = w' \quad (6.4)$$

The relations (6.2)-(6.4) will change whenever θ changes. Since the compass course is not very accurate, it may in some cases, where the instrument has an almost fixed orientation, not be regarded as necessary to correct for the course. u_n, v_n and w_n then equal u', v' and w', respectively. We define the mean values along the x_n, y_n and z_n-axis by:

$$u_m = (1/N) \cdot \sum_{i=1}^{N} u_{in} \quad (6.5)$$

$$v_m = (1/N) \cdot \sum_{i=1}^{N} v_{in} \quad (6.6)$$

$$w_m = (1/N) \cdot \sum_{i=1}^{N} w_{in} \quad (6.7)$$

This is used to estimate the angle φ between the x_n-axis and the mean stream (Fig. 16b), and the angle ψ between the x_n-y_n plane and the new x-y plane defined by the mean stream line (Fig. 16c). If the data are adjusted with the compass course, φ indicates the angle between east and the mean stream line, but if the data are not adjusted with the compass course the angle between east and

the mean stream line is given by $\pi/2-(\alpha-\varphi)$. φ and ψ are defined by:

(6.8) $\varphi = \arctan(v_m/u_m)$,

(6.9) $\psi = \arctan(w_m/\sqrt{[u_m^2+v_m^2]})$.

The velocities u_n, v_n and w_n are decomposed to a coordinate system x_1, y_1, z_1 where the x_1-axis lies in the same vertical plane as the mean stream line ,and the z_1-axis is parallel to z´ (Fig. 17). The velocities in this coordinate system are given by:

(6.10) $u_1 = u_n \cdot \cos\varphi + v_n \cdot \sin\varphi$,

(6.11) $v_1 = v_n \cdot \cos\varphi - u_n \cdot \sin\varphi$,

(6.12) $w_1 = w_n$.

The next step is to decompose the velocities along the x_1, y_1 and z_1-axis into a coordinate system x_2, y_2, z_2, where the x_2-axis is parallel to the mean stream line, and the z_2-axis which is normal to the streamline makes an angle ψ with z_1 (Fig. 17). We then get:

(6.13) $u_2 = w_1 \cdot \sin\psi + u_1 \cdot \cos\psi$,

(6.14) $v_2 = v_1$,

(6.15) $w_2 = w_1 \cdot \cos\psi - u_1 \cdot \sin\psi$.

Up to now we have only considered the tilt of the instrument in the direction of the mean flow (ψ). The instrument may also tilt in the vertical plane transversal to the mean stream direction (Fig. 18). The final coordinate system is notated x,y,z with velocities u,v,w. The x-z plane is now defined by the mean stream direction and the gravity vector, i.e. the y-axis (but not necessarily the x-axis) will be horizontal. We then get:

(6.16) $u = u_2$,

(6.17) $v = v_2 \cdot \cos\beta - w_2 \cdot \sin\beta$,

(6.18) $w = w_2 \cdot \cos\beta + v_2 \cdot \sin\beta$,

where β is the tilt angle in the transversal direction.

Unfortunately the angle β is not known, and can not be estimated from the velocity measurements. We can, however, guess at some values of β in order to investigate how sensitive the Reynolds stresses are to this tilt.

6.2. The effect of movements of the instument during measurements

During the measurements the instrument may move for two main reasons:
1) Forces from the flowing water act upon the instrument and the suspension.
2) The research vessel may move in its anchoring.

The movements of point 1 will not influence our calculated mean stream significantly because these movements are of relatively short periods (observed in the tank test), and a mean value over a record length of several oscillations will not be influenced by these movements. The movements of point 2 may influence the mean stream values if the recording period is of the same order as the period of the movements, but the effect on the mean value will be reduced if the length of the series of measurement is many times the oscillation period. The Reynolds stresses, however, will be severely influenced by such movements, so that they should be avoided at all costs.

We shall here discuss point 1 in more detail. The instrument may for instance oscillate about a horizontal axis (Fig. 19). If the movements are in the x-z plane, then this will cause fictive velocities given by:

(6.19) $u_1 = -r_1 \cdot d\theta_1/dt$, $v_1 = 0$, $w_1 = 0$.

If the oscillations are transversal to the x-z plane, that is in the y-z plane, then the fictive velocities are:

(6.20) $u_2=0$, $v_2=-r_2 \cdot de_2/dt$, $w_2=0$.

r_1 and r_2 are the curvature radii of the oscillations in the x-z and y-z planes, respectively, and e_1 and e_2 are the angles between the vertical and the instrument in the x-z and y-z planes. The instrument will also record perturbations when oscillating in the x-z plane due to the components of the mean flow U:

(6.21) $u_3=U \cdot \cos e_1 - U$, $v_3=0$, $w_3=-U \cdot \sin e_1$.

The instrument may also rotate about its vertical axis (Fig. 20). It will then record perturbations due to the components of the mean flow, given by:

(6.22) $u_4=U \cdot \cos e_3 - U$, $v_4=-U \cdot \sin e_3$, $w_4=0$,

where e_3 is the angle of rotation.

If we add together all the possible false velocity contributions described above, we get:

(6.23) $u'=-r_1 \cdot de_1/dt + U \cdot \cos e_1 - 2U + U \cdot \cos e_3$,

(6.24) $v'=-r_2 \cdot de_2/dt - U \cdot \sin e_3$,

(6.25) $w'=-U \cdot \sin e_1$.

In order to simplify the estimation of these effects on the Reynolds stresses we will first write the different angles as periodic functions:

(6.26) $e_1=a_0 \cdot \sin(\sigma_1 t+\alpha_1)$,

(6.27) $e_2=b_0 \cdot \sin(\sigma_2 t+\alpha_2)$,

(6.28) $\theta_3 = c_0 \cdot \sin(\sigma_3 t + \alpha_3)$.

To simplify further we will let θ_1, θ_2 and θ_3 have the same amplitude and frequency, but let the phase constants α_i be different:

(6.29) $a_0 \approx b_0 \approx c_0 = a$,

(6.30) $\sigma_1 \approx \sigma_2 \approx \sigma_3 = \sigma$.

Furthermore we let $r_1 \approx r_2 = r$ and make a series expansion of θ_1, θ_2 and θ_3, where all terms of order 4 or more are omitted. If we choose the phase constants so that maximum values for the Reynolds stresses are obtained, the results become:

(6.31) $\overline{u'u'} \approx \frac{1}{2}(ra\sigma)^2$,

(6.32) $\overline{u'v'} \approx \pm\frac{1}{2}a^2[r^2\sigma^2 + Ur\sigma]$,

(6.33) $\overline{u'w'} \approx 0$,

(6.34) $\overline{v'v'} \approx \frac{1}{2}a^2[r\sigma + U]^2$,

(6.35) $\overline{v'w'} \approx \pm\frac{1}{2}a^2[Ur\sigma + U^2]$,

(6.36) $\overline{w'w'} \approx \frac{1}{2}(Ua)^2$.

By inserting reasonable values in the expressions above we may see how sensitive the Reynolds stresses are to such oscillations. We have chosen U=50 cm/s, T=600 s, $\sigma = 2\pi/20$ s, $a = 2^0 = 4\pi/360$, and r=2 m. With these values we get:

$\overline{u'u'} \approx 2.4 \quad cm^2/s^2$,
$\overline{u'v'} \approx \pm 4.3 \quad cm^2/s^2$,
$\overline{u'w'} \approx 0 \quad cm^2/s^2$,
$\overline{v'v'} \approx 7.7 \quad cm^2/s^2$,
$\overline{v'w'} \approx \pm 3.4 \quad cm^2/s^2$,
$\overline{w'w'} \approx 1.5 \quad cm^2/s^2$.

We see that $\overline{u'w'}$ is the Reynolds stress which is least influenced by the movements of the instrument, while the other stresses may be more influenced. Especially the sensitivity of the terms including v' to these oscillations should be noted. The same tendency can also be read out from the tank measurements, as presented in Table 6.

7. CONCLUSIONS

The UCM-10 current meter was found suitable for turbulence measurements. Some points, however, could be improved: The temperature sensor responded too slowly to register the turbulent heat transport. The compass course was too inaccurate and too seldom registered to be fully useable. Tilt sensors would make it possible to get more accurate turbulence data, but still the instrument should move as little as possible in order to get accurate values for all the Reynolds stresses. (The new model, UCM-40, is probably improved on several of these points.) The term $\overline{u'w'}$ is, however, not so sensitive to twisting and tilting of the instrument as the other stresses. The contribution to $\overline{u'w'}$ from self-generated turbulence seems to be small for mean velocities up to 1 m/s if the vertical sensor is positioned before the instrument, towards the mean flow.

ACKNOWLEDGEMENTS

We are due thanks to Trond Guddal of Simrad Optronics who patiently has helped with our problems. We are also due thanks to the Norwegian Council for Science and the Humanities for financial support to the calibration of the instrument.

REFERENCES

Gythre,T., 1976, The use of high sensitivity ultrasonic current meter in an oceanographic aqustition system., Radio & Electr. Eng., 46, 617-623.

Kolstad,T., 1985, Calibration of UCM-10 current meter. Wadic project, pro.nr. 020360, Oceanor. Classified report.

Martinsen,T., 1988, Turbulensmålinger under is. Thesis, Inst. geophys., Univ. Oslo.

Soulsby,R.L., 1980, Selecting record length and digitization rate for near bed turbulence measurements. J. Phys. Oceanogr.,10,208-219.

Sørgård,E., 1988, Turbulensmålinger i en saltkile, Thesis, Inst. geophys., Univ. Oslo.

Sørgård,E., Martinsen,T. and Aas,E., 1988, Drag coefficient at a salt wedge, to be published.

TABLE 1

OFFSET MEASUREMENTS AT DIFFERENT TEMPERATURES

T is temperature, and u_m, v_m, w_m are mean velocities recorded by the sensors of the instrument.

T (^{0}C)	u_m (cm/s)	v_m (cm/s)	w_m (cm/s)
0.0	-1.4	-0.8	-0.6
6.6	-1.2	-0.8	-0.3
7.6	-1.0	-0.3	-0.4
8.2	-1.5	-0.5	-1.1
8.4	-1.2	-0.6	-0.9
8.5	-1.6	-0.5	-1.2
9.2	-1.5	-0.7	-1.1
9.8	-0.9	-0.4	-0.4
9.9	-1.5	-0.7	-1.4
10.6	-1.2	-0.8	-1.5
10.7	-1.2	-0.8	-1.4
10.8	-1.0	-0.4	-0.8
11.2	-0.7	-0.2	-0.5
12.1	-1.3	-0.3	-1.1
12.2	-0.7	-0.2	-0.5
12.5	-1.2	-0.9	-1.5
12.5	-1.0	-0.6	-1.2
13.1	-1.1	-0.9	-1.0
13.1	-1.5	-0.7	-1.0
13.3	-1.1	-0.8	-1.2
13.8	-1.3	-0.6	-1.2
15.1	-0.6	-0.1	-0.4
15.8	-1.0	-1.0	-1.7
15.8	-1.0	-1.1	-1.6
17.4	-1.0	-0.6	-0.9
18.4	-0.8	-0.5	-1.1
18.4	-0.8	-0.5	-1.0
19.5	-1.1	-0.5	-1.2
20.1	-1.1	-0.9	-1.0
20.1	-1.2	-0.9	-1.0
20.5	-0.8	-0.8	-0.9
21.3	-1.1	-0.6	-1.6

TABLE 2

CALIBRATION DATA FOR THE VERTICAL VELOCITY SENSOR

W and w_m are true and measured mean velocities, respectively. Δp is pressure and t is time used by the sensor at the distance corresponding to Δp.

Δp (10^5 Pa)	t (s)	W (cm/s)	w_m (cm/s)
2.02	126	16.0	10.1
-2.00	142	-14.1	-4.9
2.01	60	33.5	19.7
-1.98	70	-28.3	-15.9
2.04	46	44.3	24.6
-1.97	53	-37.2	-21.7
2.01	35	57.4	35.3
-1.96	37	-53.0	-31.8
1.88	20	94.0	46.1
-1.94	18	-107.8	-56.7
2.03	221	9.2	4.7
-2.00	249	-8.0	- 4.7

TABLE 3

CALIBRATION DATA FOR THE HORIZONTAL VELOCITY SENSORS

U_l is the speed of the lorry, u_m, v_m, w_m are mean velocities recorded by the different sensors. U,V and W are true values. Index 1 refers to start values, index 5 to the values after 4 times of successive approximations. φ is the angle between the x-axis and the mean flow. Angles are in degrees and velocities in cm/s.

U_l	u_m	v_m	w_m	U_1	V_1	W	φ_1	U_5	V_5	φ_5
5	1.9	-2.1	0.8	3.2	-3.6	1.3	5.45	3.2	-3.6	312.3
10	3.7	-4.5	1.2	6.2	-7.6	2.1	5.40	6.2	-7.6	309.4
15	5.2	-6.6	1.5	9.1	-11.6	2.6	5.38	9.1	-11.6	308.3
20	9.6	-9.8	1.9	13.9	-14.1	3.2	5.49	13.9	-14.1	314.6
30	15.5	-15.8	2.3	20.8	-21.2	4.0	5.49	20.9	-21.2	314.6
40	23.5	-23.2	2.0	28.4	-28.0	3.4	5.50	28.3	-28.1	315.1
50	30.5	-29.9	1.8	35.6	-34.9	3.1	5.51	35.6	-35.0	315.7
60	38.4	-39.2	1.3	42.0	-42.8	2.1	5.49	42.1	-42.7	314.6
70	50.3	-48.3	-1.1	50.5	-48.5	-1.8	5.52	50.2	-48.7	315.7
80	59.3	-58.1	-2.4	57.1	-55.9	-4.1	5.51	57.0	-56.0	315.7
90	64.1	-68.2	-6.5	61.2	-65.1	-11.1	5.47	61.6	-64.7	313.4
100	70.5	-73.7	-11.4	67.8	-70.9	-19.4	5.48	68.1	-70.6	314.0
150	79.3	-84.3	-63.7	71.7	-75.6	-108.4	5.47	70.3	-76.3	312.8
20	11.0	-8.4	1.5	15.8	-12.0	2.5	5.63	15.7	-12.2	322.0
40	22.0	-23.0	1.7	27.5	-28.9	3.0	5.47	27.7	-28.7	314.0
60	39.6	-39.3	0.1	42.6	-42.3	0.2	5.50	42.5	-42.3	315.1
80	56.6	-59.4	-3.2	55.1	-57.8	-5.4	5.47	55.4	-57.5	314.0
100	68.9	-72.7	-10.5	67.7	-71.4	-17.9	5.47	68.1	-71.1	314.0
150	81.8	-85.5	-59.7	76.4	-79.9	-101.4	5.48	75.7	-80.5	313.4
15	2.4	-10.1	0.0	3.5	-14.6	0.0	4.95	3.5	-14.6	283.6
30	4.2	-22.5	-0.8	5.5	-29.5	-1.3	4.90	6.8	-29.2	283.0
5	2.0	2.4	0.3	3.2	3.8	0.6	0.87	3.2	3.8	49.9
10	3.5	4.5	0.0	6.1	7.9	0.0	0.91	6.1	7.9	52.1
15	5.0	8.2	-0.2	7.8	12.8	-0.4	1.03	7.8	12.8	59.0
20	7.0	13.0	-0.6	9.4	17.6	-1.0	1.08	10.0	17.3	60.2
30	13.7	20.3	-1.2	16.7	24.8	-2.1	0.98	17.9	24.0	53.3
40	16.9	28.6	-1.8	20.3	34.3	-3.1	1.04	21.9	33.3	56.7
50	22.9	38.3	-2.3	25.6	42.8	-3.9	1.03	27.4	41.7	56.7
60	27.3	49.6	-2.7	28.8	52.4	-4.6	1.07	31.8	50.7	57.9
70	31.7	60.2	-2.9	32.5	61.8	-5.0	1.09	36.5	59.5	58.4
80	38.9	69.7	-3.5	38.9	69.7	-6.0	1.06	43.1	67.2	57.3
90	39.1	7.5	-3.9	40.4	80.1	-6.6	1.10	45.6	77.3	59.6
100	41.2	85.3	-4.4	43.4	89.8	-7.4	1.12	47.7	87.6	61.3
150	29.7	133.5	-13.2	32.3	144.8	-22.5	1.35	34.6	144.2	76.8
50	-22.3	-34.7	-1.7	-27.0	-42.0	-2.9	4.14	-28.4	-41.1	235.5
20	-6.0	-13.1	-0.1	-8.3	-18.2	-0.1	4.28	-8.9	-17.9	243.5

TABLE 4

CALIBRATION DATA FOR THE TEMPERATURE SENSOR

t_m is measured mean temperature and T is true temperature, both in degree Celsius.

T	t_m
0.0	-0.2
8.5	8.3
9.7	9.5
10.6	10.4
10.7	10.6
10.7	10.5
12.0	11.9
15.8	15.6
17.3	17.2
18.4	18.2
21.2	21.1

TABLE 5

CALIBRATION DATA FOR THE SALINITY SENSOR

V is the volume of water in the vessel. V_2 is the volume of salt water removed with density ϱ_1, and V_3 the volume of the fresh water added with density ϱ_3. S_m is measured mean salinity, and S the true salinity. All volumes are in dm^3, density in kg/m^3, and salinity in practical salinity units.

V	V_2	V_3	ϱ_3	ϱ_1	S	S_m
36	-	-	998	1024	34.55	32.62
36	4	4	998	1021	30.80	29.30
36	4	4	998	1019	27.44	26.17
36	4	4	998	1017	24.45	23.09
36	4	4	998	1014	21.78	20.48
36	4	4	998	1013	19.39	18.17
36	4	4	998	1011	17.27	16.06
36	4	4	998	1010	15.37	14.13
36	4	4	998	1008	13.68	12.42
36	6	6	998	1007	11.42	10.05
36	6	6	998	1005	9.53	8.07
36	8	8	998	1003	7.42	5.79
36	10	10	998	1002	5.37	3.63
36	14	14	998	1000	3.29	1.48

TABLE 6

TURBULENCE MEASURED IN STILL WATERS AT DIFFERENT SPEEDS

u′,v′,w′ are perturbation velocities. u′ is velocity in the direction of the mean flow, v′ in the transversal direction, and w′ upwards. U is the velocity of the mean flow. All velocities are in cm/s and the correlations in cm^2/s^2.

series	U	$\overline{u'u'}$	$\overline{u'v'}$	$\overline{u'w'}$	$\overline{v'v'}$	$\overline{v'w'}$	$\overline{w'w'}$
A	4.6	0.36	0.11	-0.05	0.25	-0.03	0.20
A	9.2	0.15	0.03	-0.01	0.17	0.00	0.13
A	12.9	0.27	0.15	-0.05	0.32	-0.03	0.10
A	20.6	0.58	0.87	-0.10	8.23	-0.52	0.15
A	29.8	0.20	0.08	-0.03	0.43	-0.05	0.25
A	40.2	0.30	0.30	-0.05	1.26	-0.10	0.12
A	49.8	0.69	0.56	-0.11	21.63	-2.15	0.36
A	60.6	0.78	-0.31	-0.06	10.06	-0.98	0.28
A	72.2	1.10	-1.35	-0.07	7.88	-0.93	0.34
A	82.7	0.73	-0.35	-0.09	1.61	-0.06	0.30
A	91.5	0.99	0.32	-0.23	1.09	-0.03	0.57
A	99.3	0.82	0.19	-0.34	0.77	-0.08	0.93
A	154.4	3.47	-1.51	2.76	7.68	-1.37	6.85
B	20.7	0.34	-0.17	-0.03	1.07	0.01	0.16
B	39.1	0.66	1.03	-0.11	3.81	-0.32	0.20
B	61.3	0.46	-0.34	-0.06	3.80	-0.25	0.35
B	82.0	1.04	0.10	-0.05	1.12	-0.02	0.25
B	97.6	0.67	0.06	-0.19	0.68	0.10	0.90
B	151.9	3.75	0.66	3.41	7.37	1.14	6.34
C	15.3	2.41	-5.46	-0.03	17.11	0.26	0.32
C	28.3	0.10	0.04	-0.02	0.36	0.01	0.28
D	4.7	0.08	-0.01	0.02	0.08	0.01	0.17
D	8.5	0.13	-0.05	0.01	0.16	0.00	0.09
D	14.5	0.74	0.19	-0.01	0.22	0.01	0.10
D	21.1	0.16	-0.10	-0.02	0.20	0.03	0.19
D	31.7	0.40	0.15	-0.05	0.16	0.01	0.15
D	40.3	0.56	0.10	-0.07	0.21	0.00	0.22
D	51.0	0.45	-0.01	0.00	0.26	0.01	0.10
D	60.8	0.51	0.02	-0.02	0.35	0.04	0.19
D	70.1	1.50	-0.26	0.08	4.72	0.13	0.23
D	78.3	0.96	-2.93	0.06	14.24	0.02	0.40
D	85.0	1.56	-4.83	0.13	22.45	-0.37	0.35
D	93.5	1.11	0.20	0.29	38.03	0.10	0.40
D	149.8	3.91	2.44	2.42	19.09	0.18	3.49
E	20.4	0.45	-0.04	-0.07	0.33	-0.01	0.48
E	48.1	10.77	-0.44	-1.86	0.36	-0.05	1.07

Fig. 1

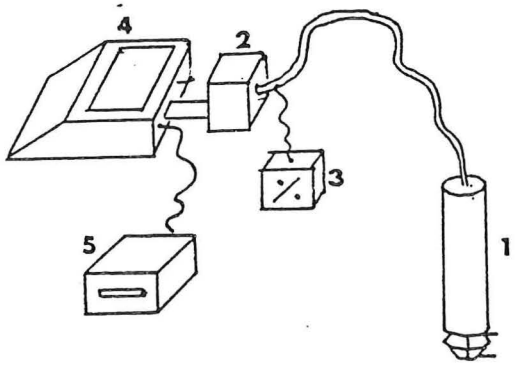

The setting up for measurements: (1) Current meter, (2) interface, (3) Power supply, (4) Micro computer, (5) Diskette station.

Fig. 2a

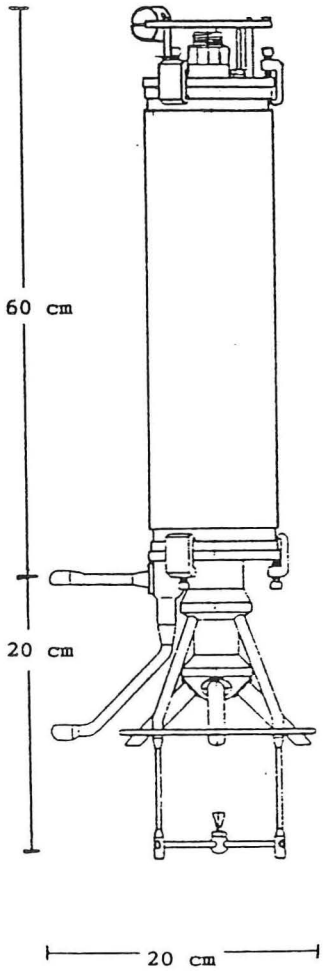

The ultrasonic current meter UCM-10

Fig. 2b

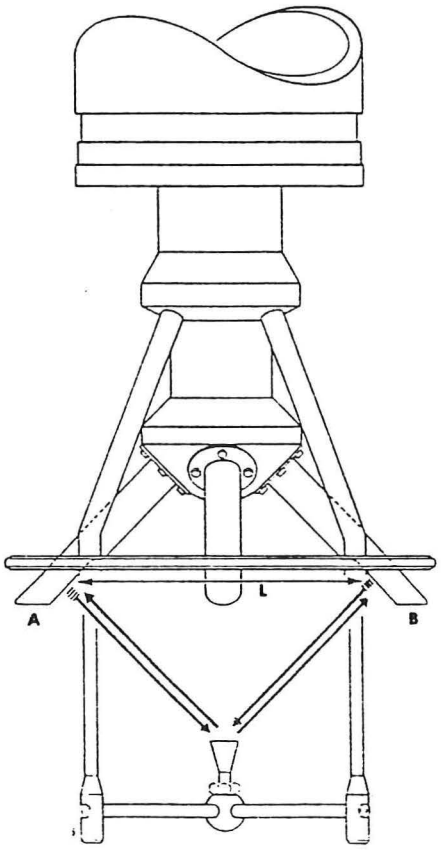

The acoustic wave path from transducer to receiver

Fig. 3

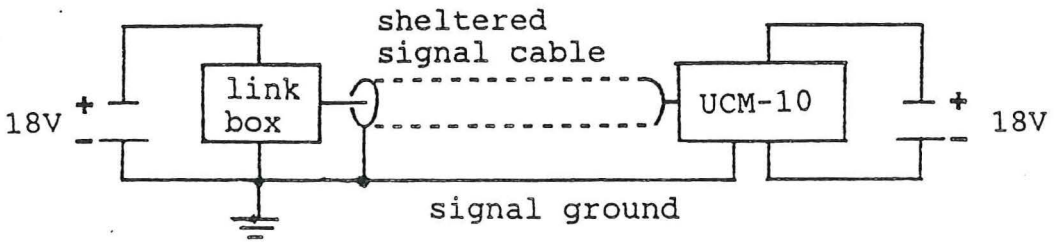

Diagram of connections for power supply and signal ground.

Fig. 4a

Offset measurements for u at different temperatures.

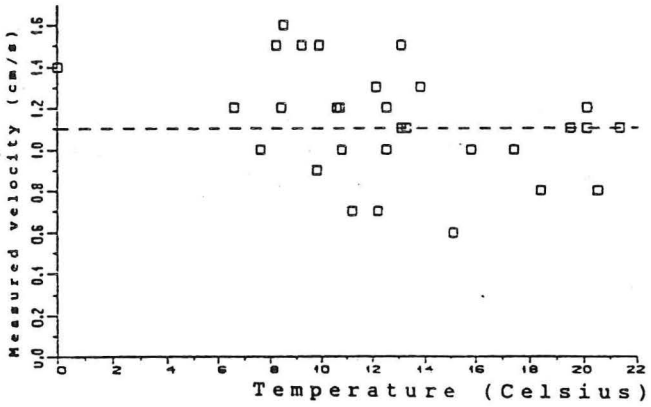

Fig. 4b

Offset measurements for v at different temperatures.

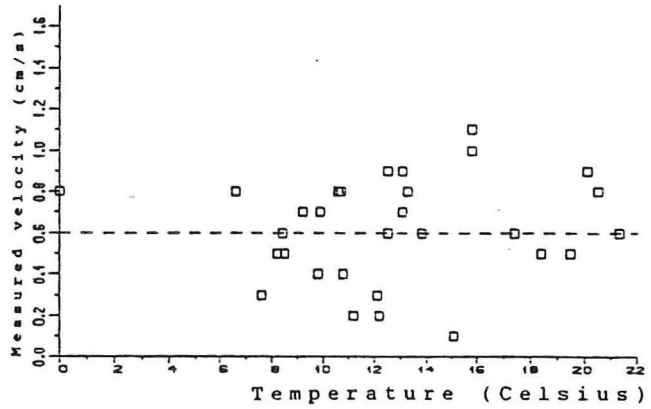

Fig. 4c

Offset measurements for w at different temperatures.

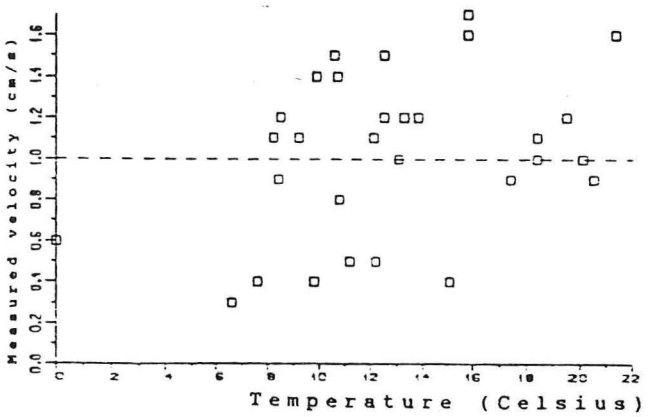

Fig. 5a

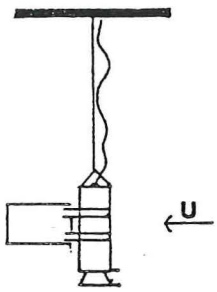

Fig. 5b

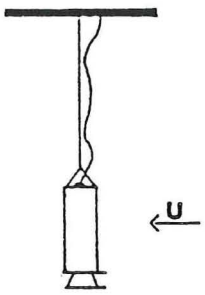

Fig. 5c

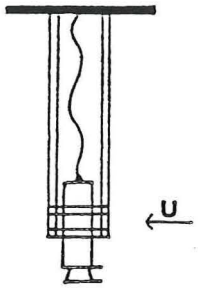

The different suspensions of the tank test.

Fig. 6a

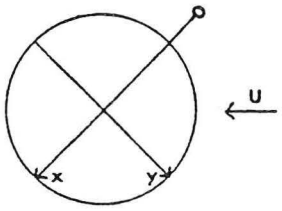

Fig. 6b

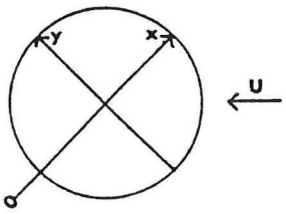

The position of the vertical velocity sensor relative to the mean stream.

Fig. 7

Calibration data and curve for the vertical velocity sensor.

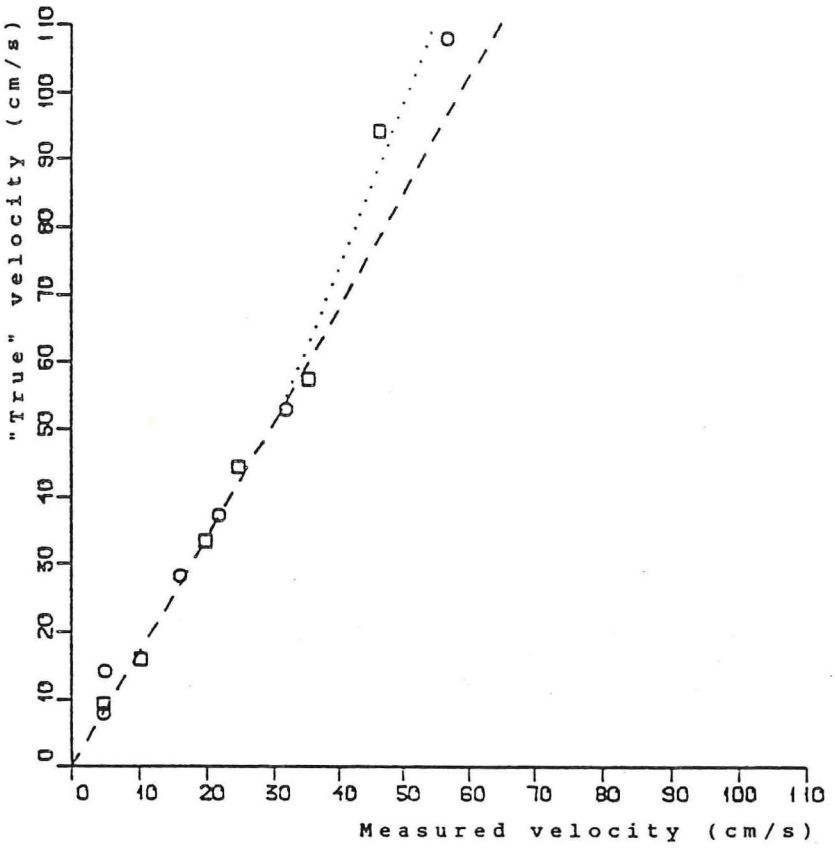

Fig. 8

Calibration curve for the horizontal velocity sensors when taking into account the two largest values for the vertical velocity.

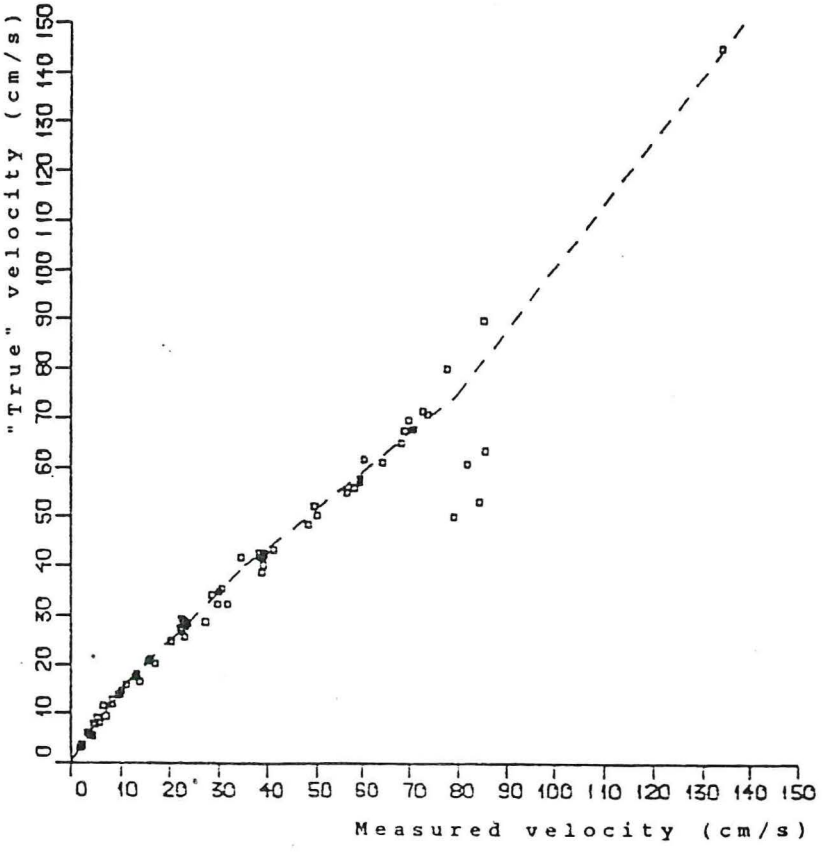

Fig. 9

Error in the horizontal velocities due to an inaccurate angle φ.

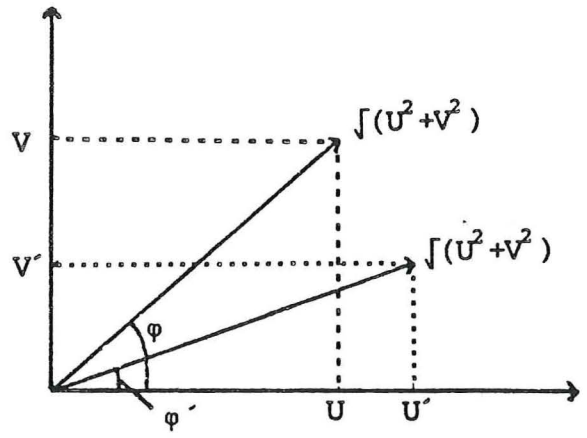

φ´ : calculated angle.
φ : "true" angle.
U´,V´ : calculated "true" velocity.
U ,V : "true" velocity.

Fig. 10

Calibration data and curve for the horizontal velocity sensors after the successive approximations.

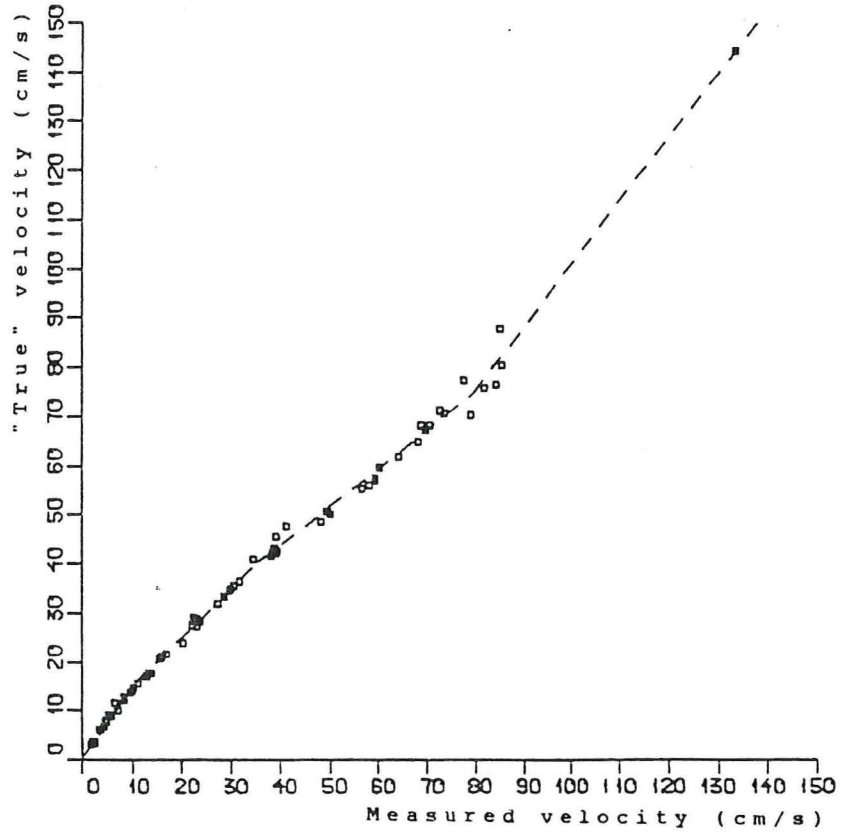

Fig. 11

Calibration data and curve for the temperature sensor.

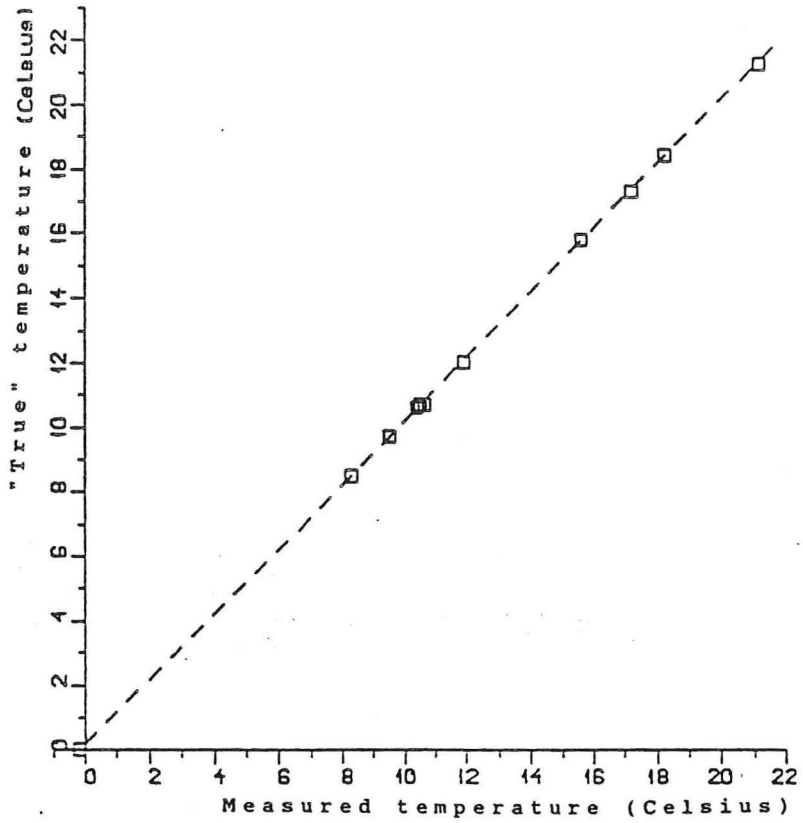

Fig. 12

Calibration data and curve for the salinity sensor at 20 °C.

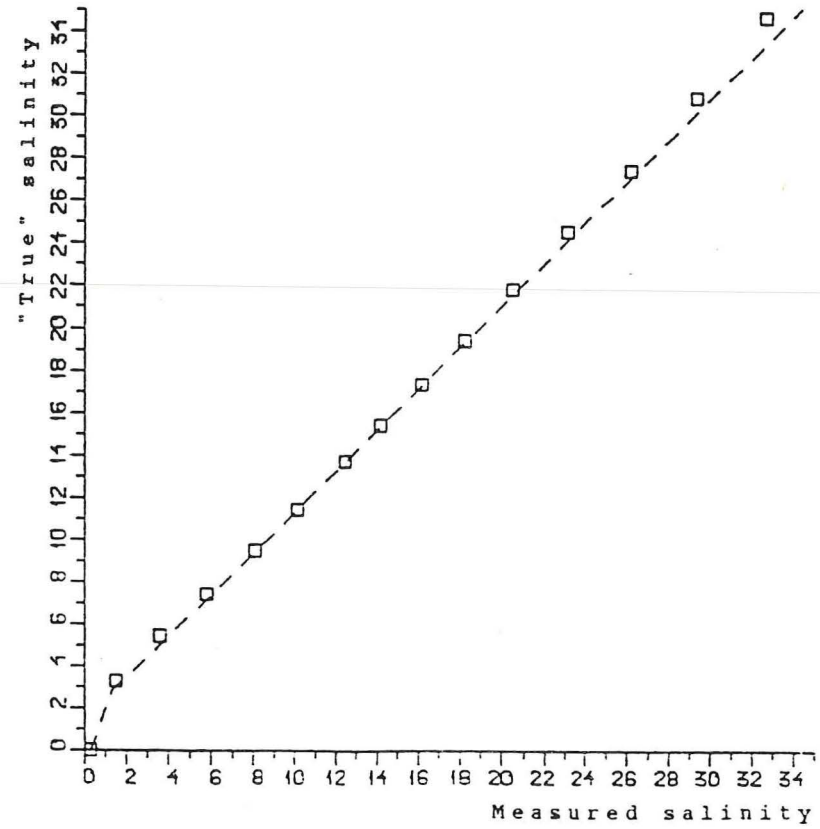

Fig. 13

$\overline{u'w'}$ recorded in still waters at different speeds of the instrument.

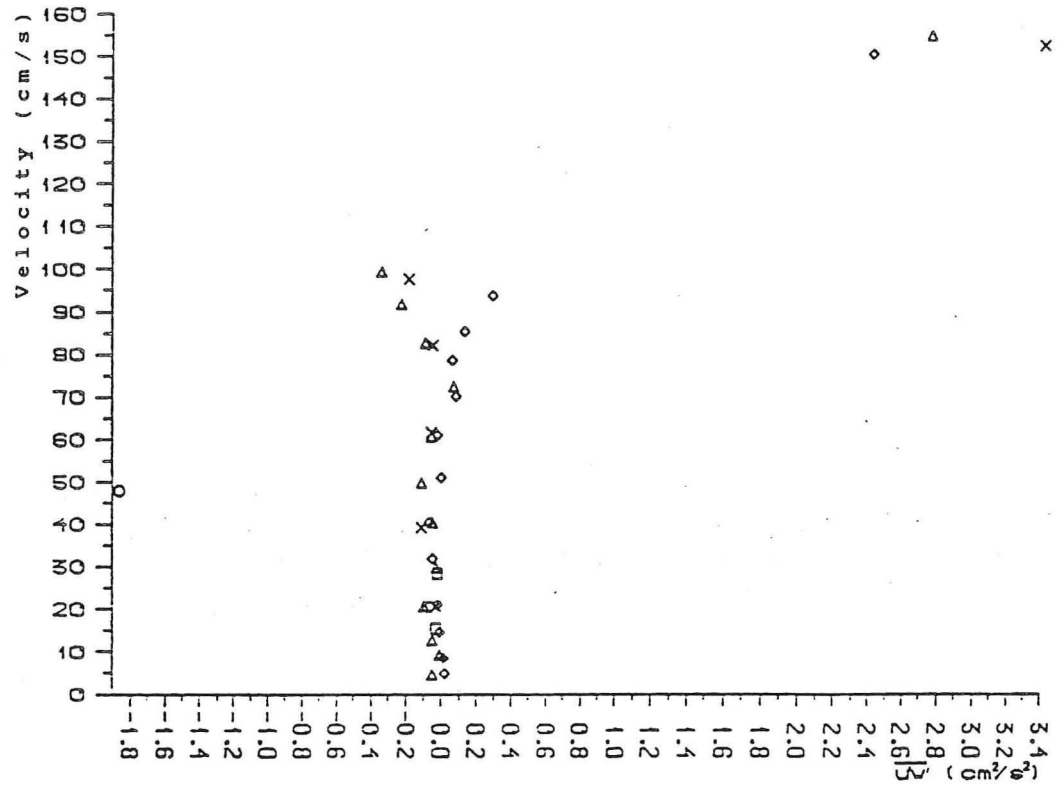

Fig. 14

$\overline{u'w'}$ recorded in still waters at different speeds of the instrument .

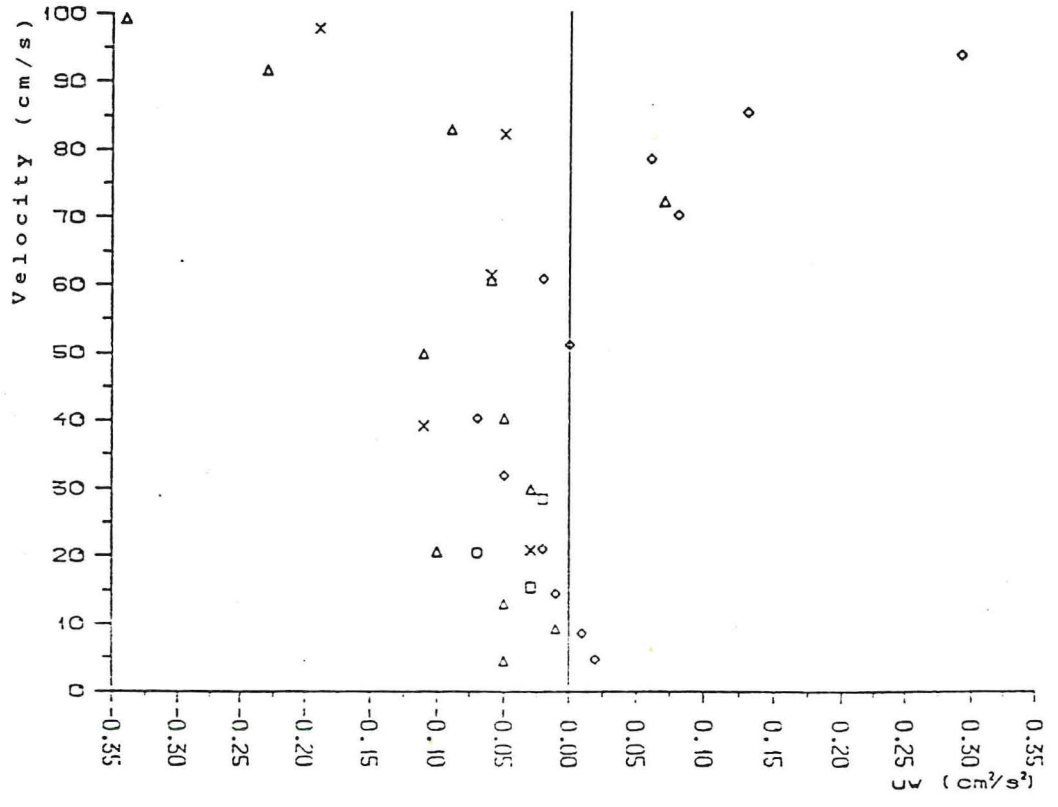

'Δ', '×', '□', '◇', and 'O' are series A,B,C,D and E respectively.

Fig. 15

Tilt of the instrument in the direction of the mean flow and in the transversal direction.

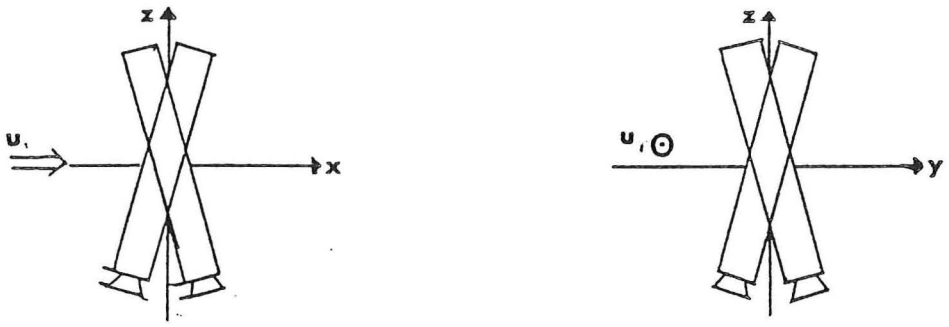

Fig. 16a

Velocities defined relative to magnetic north.

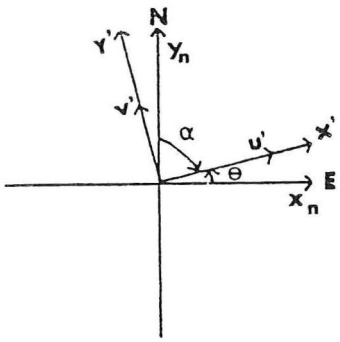

Fig. 16b

The x_n-axis defined relative to the mean stream.

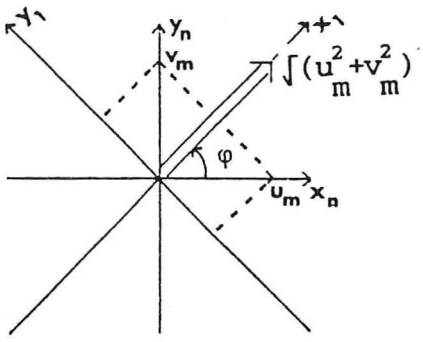

Fig. 16c

Definition of the angle between the instrument and the mean stream.

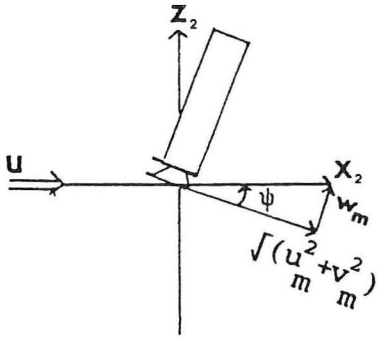

Fig. 17

Definition of the x_1 and x_2-axis relative to the mean stream line. The x_2-axis is parallel to the mean stream line.

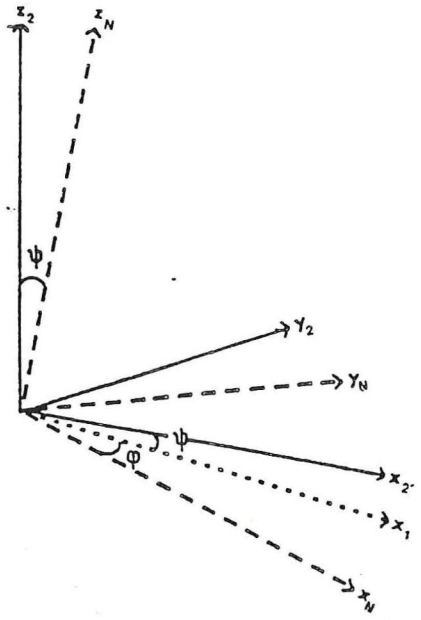

Fig. 18

The transversal tilt of the sensor.

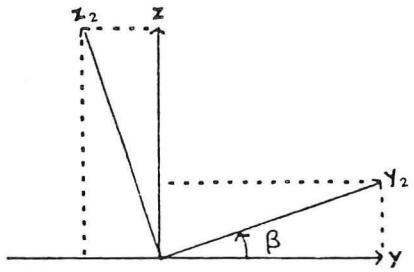

Fig.19

The oscillation angles Θ_1 and Θ_2 of the instrument.

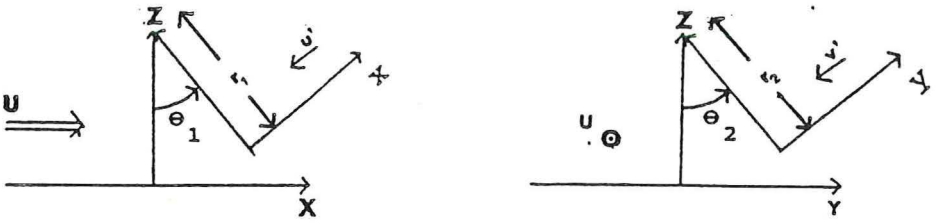

Fig. 20

The angle of rotation Θ_3 of the instrument.